Exploratory Evaluation of MR Permeability with ^{18}F-FDG PET Mapping in Pediatric Brain Tumors: A Report from the Pediatric Brain Tumor Consortium

Katherine A. Zukotynski[1,2], Frederic H. Fahey[2,3], Sridhar Vajapeyam[3], Sarah S. Ng[3], Mehmet Kocak[4], Sridharan Gururangan[5], Larry E. Kun[6], and Tina Y. Poussaint[2,3]

[1]Department of Medical Imaging, Sunnybrook Health Sciences Centre, University of Toronto, Toronto, Ontario, Canada; [2]Department of Radiology, Harvard Medical School, Boston, Massachusetts; [3]Department of Radiology, Boston Children's Hospital, Boston, Massachusetts; [4]Department of Biostatistics, St. Jude Children's Research Hospital, Memphis, Tennessee; [5]Department of Radiology, Duke University Medical Center, Durham, North Carolina; and [6]Department of Radiological Sciences, St. Jude Children's Research Hospital, Memphis, Tennessee

The purpose of this study was to develop a method of registering ^{18}F-FDG PET with MR permeability images for investigating the correlation of ^{18}F-FDG uptake, permeability, and cerebral blood volume (CBV) in children with pediatric brain tumors and their relationship with outcome. **Methods:** Twenty-four children with brain tumors in a phase II study of bevacizumab and irinotecan underwent brain MR and ^{18}F-FDG PET within 2 wk. Tumor types included supratentorial high-grade astrocytoma (n = 7), low-grade glioma (n = 9), brain stem glioma (n = 4), medulloblastoma (n = 2), and ependymoma (n = 2). There were 33 cases (pretreatment only [n = 12], posttreatment only [n = 3], and both pretreatment [n = 9] and posttreatment [n = 9]). ^{18}F-FDG PET images were registered to MR images from the last time point of the T1 perfusion time series using mutual information. Three-dimensional regions of interest (ROIs) drawn on permeability images were automatically transferred to registered PET images. The quality of ROI registration was graded (1, excellent; 2, very good; 3, good; 4, fair; and 5, poor) by 3 independent experts. Spearman rank correlations were used to assess correlation of maximum tumor permeability (Kps_{max}), maximum CBV (CBV_{max}), and maximum ^{18}F-FDG uptake normalized to white matter (T/W_{max}). Cox proportional hazards models were used to investigate associations of these parameters with progression-free survival (PFS). **Results:** The quality of ROI registration between PET and MR was good to excellent in 31 of 33 cases. There was no correlation of baseline Kps_{max} with CBV_{max} (Spearman rank correlation = 0.018 [P = 0.94]) or T/W_{max} (Spearman rank correlation = 0.07 [P = 0.76]). Baseline CBV_{max} was correlated with T/W_{max} (Spearman rank correlation = 0.47 [P = 0.036]). Baseline Kps_{max}, CBV_{max}, and T/W_{max} were not significantly associated with PFS (P = 0.42, hazard ratio [HR] = 0.97, 95% confidence interval [CI] = 0.90–1.045, and number of events [n_{events}] = 15 for Kps_{max}; P = 0.41, HR = 0.989, 95% CI = 0.963–1.015, and n_{events} = 14 for CBV_{max}; and P = 0.17, HR = 1.49, 95% CI = 0.856–2.378, and n_{events} = 15 for T/W_{max}). **Conclusion:** ^{18}F-FDG PET and MR permeability images were successfully registered and compared across a spectrum of pediatric brain tumors. The lack of correlation between metabolism and permeability may be expected because these parameters characterize different molecular processes. The correlation of CBV and tumor metabolism may be related to an association with tumor grade. More patients are needed for a covariate analysis of these parameters and PFS by tumor histology.

Key Words: MR permeability; cerebral blood volume; ^{18}F-FDG PET; pediatric; brain tumor

J Nucl Med 2013; 54:1237–1243
DOI: 10.2967/jnumed.112.115782

In the evaluation of pediatric brain tumors, MR imaging is diagnostic for defining anatomic tumor extent but is limited in evaluating tumor physiology. More recently, advanced MR imaging techniques have been used to characterize tumors in functional and metabolic terms. PET with ^{18}F-FDG is used as a tool to demonstrate metabolically active disease and to complement anatomic imaging in these children. Initial studies of ^{18}F-FDG PET in children with brain tumors highlighted the heterogeneity of uptake across the spectrum of disease (*1*). Several studies have suggested that more intensely ^{18}F-FDG–avid disease or more extensive ^{18}F-FDG uptake is associated with a higher histologic grade and worse outcome (*1–11*). In 2008, Williams et al. evaluated 3-dimensional (3D) methods of ^{18}F-FDG PET quantification in pediatric anaplastic astrocytoma and concluded that using a 3D volume of interest yielded an estimate of metabolically active tumor burden and was related to survival (*11*). More recently, we described findings in ^{18}F-FDG PET studies in pediatric diffuse intrinsic brain stem glioma (BSG) and included the association of ^{18}F-FDG PET with MR imaging metrics (*12*). The correlation of tumor metabolism and perfusion metrics using the combination of ^{18}F-FDG PET with MR permeability could provide a more complete understanding of tumor biology and aggressiveness, resulting in an improved ability to determine prognosis and therapy response, compared with ^{18}F-FDG PET or MR permeability alone. Although PET/CT and MR imaging scanners are common, PET/MR is relatively rare in routine clinical practice. A practical approach is needed for combining ^{18}F-FDG PET with MR permeability images after independent acquisition with good to excellent coregistration of the tumor region of interest (ROI).

Received Oct. 16, 2012; revision accepted Apr. 2, 2013.
For correspondence or reprints contact: Tina Young Poussaint, Department of Radiology, Boston Children's Hospital, 300 Longwood Ave., Boston, MA 02115.
E-mail: tina.poussaint@childrens.harvard.edu
Published online Jun. 25, 2013.

The aim of this study was to evaluate the feasibility of registering ^{18}F-FDG PET with MR permeability images using a common ROI that could be applied to both neuroimaging modalities, to investigate the correlation between these studies in pediatric brain tumors and to assess relationships between PET and MR metrics with progression-free survival (PFS). A 3D ROI on MR permeability images that could be applied to ^{18}F-FDG PET images was explored to noninvasively assess different aspects of tumor physiology including perfusion and metabolism.

MATERIALS AND METHODS

Study Description

The Pediatric Brain Tumor Consortium (PBTC) is a multidisciplinary cooperative research organization of 11 institutions involved in testing novel therapies for children with primary central nervous system tumors. Ten of the 11 institutions have PET imaging capabilities and were included in this study. The institutional review boards of each PBTC institution approved the study before initial patient enrollment, and continuing approval was maintained throughout the study. Patients or their legal guardians gave written informed consent, and assent was obtained, as appropriate, at the time of enrollment. Through a multiinstitutional clinical trial for children with recurrent brain tumors, 24 children in a phase II study of bevacizumab (Avastin; Genentech Corp.) and irinotecan (Camptosar; Pfizer Corp.) underwent both brain MR imaging and ^{18}F-FDG PET within 2 wk of each other. In total, 33 cases of concurrent MR and ^{18}F-FDG PET were available: 12 children underwent pretreatment MR and ^{18}F-FDG PET only (12 cases), 3 children underwent posttreatment MR and ^{18}F-FDG PET only (3 cases), and 9 children underwent both pretreatment and posttreatment MR and ^{18}F-FDG PET (18 cases). Tumor types included supratentorial high-grade glioma (HGG; $n = 7$), low-grade glioma (LGG; $n = 9$), BSG ($n = 4$), medulloblastoma ($n = 2$), and ependymoma ($n = 2$). All images acquired at participating institutions were transferred to the PBTC Operations and Biostatistics Center and then the PBTC Neuroimaging Center for evaluation (*13*).

^{18}F-FDG PET and MR Acquisition

^{18}F-FDG PET scans were acquired on a variety of scanners (Advance NXI [GE Healthcare], Discovery LS [GE Healthcare], Discovery STE [GE Healthcare], G-PET [Philips], HR1 [Siemens], and HiRez Bioscan [Siemens]). The consistency of the PET data was maintained by adherence to a standard acquisition protocol and quality assurance program, which included daily blank scans and quarterly normalization, calibration, and preventive maintenance (*14*). Patients fasted for 4 h before PET. The baseline brain PET scan was acquired in 3D mode for 10 min at 40–60 min after the intravenous administration of ^{18}F-FDG (5.55 MBq/kg) (minimum dose, 18 MBq; maximum dose, 370 MBq). Attenuation correction was performed using a 3-min segmented transmission scan with ^{68}Ge/^{68}Ga rods when the scanner was PET only or a CT-based approach when images were acquired on a PET/CT scanner. The acquired data were reconstructed using Fourier rebinning, followed by a 2-dimensional ordered-subset expectation maximum reconstruction algorithm.

All MR imaging was performed on a 1.5-T scanner and included standard MR imaging with gadolinium and perfusion and diffusion images of the brain. MR T1 permeability was assessed using dynamic T1-weighted 3D spoiled gradient-recalled images, fast low-angle shot MR imaging, fast field echo with a minimum resolution of $128 \times 128 \times 16$, a 24-cm field of view, minimum repetition and echo times, a flip angle of 30°, and a repetition of 40 (using a multiphase/dynamics option). Kinetic modeling of the dynamic signal changes yielded estimates of regional fractional blood volume and microvascular permeability (Kps), a sensitive indicator of blood–brain barrier disruption and a correlate of angiogenesis. As with PET, consistency between institutions was maintained by adherence to standard quality assurance programs (*15*).

Image Analysis

All ^{18}F-FDG PET and MR images were transferred to the PBTC Neuroimaging Center for retrospective analysis. Permeability maps were computed for each brain MR study using in-house software developed using IDL (Exelis; Visual Information Solutions). The ^{18}F-FDG PET image set was registered with the raw MR image set from the last time point of the T1 perfusion time series data on a Hermes workstation (Hermes Medical Solutions) using a mutual information method with the PET data resampled along the planes of the MR image. For each case, the quality of the image registration was assessed subjectively based on the alignment of the cortical surface and gray matter. In studies where the registration was not adequate, ^{18}F-FDG PET images were registered with the T1 postcontrast anatomic images, and then the T1 postcontrast images were registered with the T1 perfusion raw data. Three-dimensional ROIs were manually drawn on the permeability images in areas of increased permeability using ImageJ (U.S. National Institutes of Health) and automatically transferred to the registered ^{18}F-FDG PET images. If there was more than one area of increased permeability on the MR image, a separate ROI was drawn for each. Only the ROI with the highest permeability was saved. Separate ROIs were drawn on the registered PET images for areas of normal white matter (contralateral centrum semiovale) to normalize the PET data.

The quality of registration of the PET and MR permeability images (including the 3D ROI) was independently assessed by 3 experts and subjectively graded on a 5-point scale (1, excellent; 2, very good; 3, good; 4, fair; and 5, poor). For each case, the quality of the image registration was assessed and based on the alignment of the cortical surface and gray matter as well as on the alignment of the tumor site and its surrounding regions. Using the 3D ROI, we recorded the maximum tumor permeability (Kps_{max}), maximum tumor cerebral blood volume (CBV_{max}), and maximum tumor ratio on ^{18}F-FDG PET (maximum pixel value in the 3D ROI normalized by white matter, T/W_{max}). In 1 child, although the MR permeability could be assessed, the cerebral blood volume (CBV) could not.

Statistical Analysis

The ^{18}F-FDG uptake ratio (T/W_{max}) on PET was correlated with the Kps_{max} and CBV_{max} on MR using Spearman rank correlation. Cox proportional hazards models were used to investigate the associations of Kps_{max}, CBV_{max}, and T/W_{max} with PFS where disease stratification of high-grade glioma (HGG)/BSG versus other histologies was used. The time to progression was calculated from the date of starting therapy to the date of progression or death. Patients who had not progressed or died at the time of their last follow-up were censored.

RESULTS

In 24 children with brain tumors, 33 cases of concurrent MR and ^{18}F-FDG PET were available for review: 12 children underwent pretreatment MR and ^{18}F-FDG PET only (12 cases), 3 children underwent posttreatment MR and ^{18}F-FDG PET only (3 cases), and 9 children underwent both pretreatment and posttreatment MR and ^{18}F-FDG PET (18 cases). Thirty-one of 33 cases (94%) had good to excellent registration of the ^{18}F-FDG PET and MR permeability images including the 3D ROI. Further, the correlation was good to excellent across a spectrum of brain tumor histologies irrespective of anatomic variations caused by the patients' disease (recurrent diffuse intrinsic BSG in Fig. 1 and glioblastoma multiforme illustrated in Fig. 2).

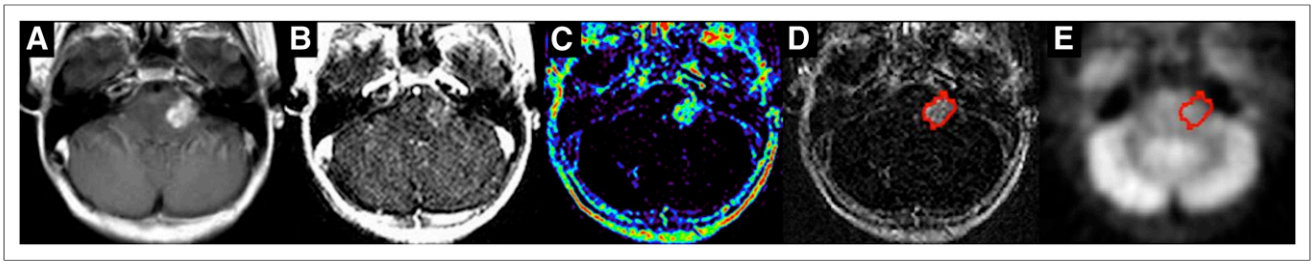

FIGURE 1. A 12-y-old girl with recurrent diffuse intrinsic BSG who relapsed during treatment. Images shown are from baseline T1 contrast-enhanced MR image (A), T1 permeability image (B), T1 permeability map (C) (Kps_{max}, 7.799), T1 permeability registered with ^{18}F-FDG PET study (D) (registration grade, excellent), and ^{18}F-FDG PET studies (E) (T/W_{max}, 1.957).

Twenty-one (12 + 9) children underwent pretherapy baseline ^{18}F-FDG PET and MR imaging studies (Table 1). Tumor types included supratentorial HGG (n = 6), BSG (n = 4), medulloblastoma (n = 2), ependymoma (n = 2), and LGG (n = 7). There was no correlation of baseline Kps_{max} with T/W_{max} (Spearman rank correlation = 0.07 [P = 0.76]) across all tumor histologies. Baseline Kps_{max} was not significantly associated with CBV_{max} (Spearman rank correlation = 0.018 [P = 0.94]), whereas baseline CBV_{max} was significantly associated with T/W_{max} (Spearman rank correlation = 0.47 [P = 0.036]). Although the numbers are too small for reliable statistical analysis, subjectively supratentorial HGG had a slightly higher correlation of Kps_{max} with T/W_{max} than LGG. When the cohort of all children with HGG/BSG was compared with the cohort of all children with LGG, there was no statistically significant difference in Kps_{max} or T/W_{max}. There was, however, the suggestion of a higher CBV_{max} (P = 0.081) in children with HGG and BSG (Table 2).

Because all the patients were alive at the time of their last follow-up, there was no analysis for overall survival. Baseline Kps_{max} was not significantly associated with PFS (P = 0.42, hazard ratio [HR] = 0.97, 95% CI = 0.90–1.045, and number of events [n_{events}] = 15) as illustrated in Figure 3A. Baseline CBV_{max} was not significantly associated with PFS (P = 0.41, HR = 0.989, 95% CI = 0.963–1.015, and n_{events} = 14) as illustrated in Figure 3B. Similarly, T/W_{max} was not significantly associated with PFS (P = 0.17, HR = 1.49, 95% CI = 0.856–2.378, and n_{events} = 15) as illustrated in Figure 3C. There was insufficient data to evaluate PFS according to histologic tumor subtype or to perform a multivariate analysis involving the 3 imaging parameters.

Only 9 patients underwent both pretherapy and posttherapy PET and MR imaging studies. Except for 1 child, all patients demonstrated a decline in both Kps_{max} and T/W_{max} when pretherapy and on-therapy scans were compared (Table 3). The extent of decrease was variable across the spectrum of tumor types. Because of the small sample size and mixture of diagnoses, it was difficult to perform a meaningful statistical analysis on this subset of patients.

DISCUSSION

A comprehensive assessment of tumor anatomy and physiology often involves spatial correlation of imaging acquired on separate MR and PET scanners. MR imaging with contrast has high soft-tissue resolution, multiplanar capability, and lack of ionizing radiation, making it the modality of choice for determining tumor size, location, and characterization. MR permeability and ^{18}F-FDG PET are advanced imaging techniques that assess different physiologic parameters and can be combined to provide insight into tumor physiology and complement anatomic information given by standard MR (T1, T2, fluid-attenuated inversion recovery, and postgadolinium T1) images. Further, MR and PET can both be used to assess tumor response or progression and to monitor treatment effects.

In clinical practice, the visual comparison of MR and brain ^{18}F-FDG PET images placed side by side is often used to subjectively coregister images. Previous work in adults has evaluated the registration of MR diffusion images with PET images; however, no common ROI was applied to either study. For example, Palumbo et al. coregistered MR diffusion and PET images with ROIs independently drawn on MR and PET using MRIcro

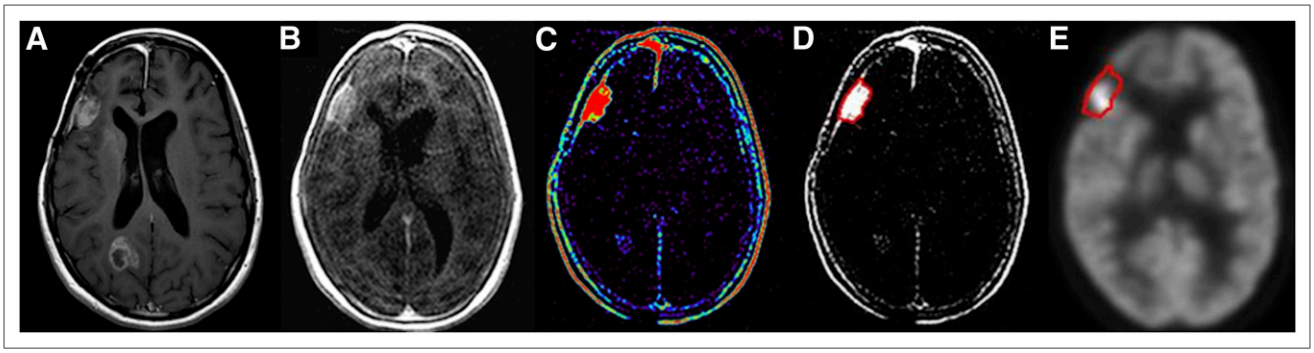

FIGURE 2. A 17-y-old girl with glioblastoma multiforme who relapsed during active treatment. Images shown are from baseline T1 contrast-enhanced MR image (A), T1 permeability image (B), T1 permeability map (C) (Kps_{max}, 27.539), T1 permeability registered with ^{18}F-FDG PET study (D) (registration grade, excellent), and ^{18}F-FDG PET studies (E) (T/W_{max}, 8.788).

TABLE 1
Summary of Tumor Histology, MR, and PET Parameters at Baseline and on Therapy

Data	*n*	Percentage	Median	Range
Male	11	46		
Female	13	54		
Recurrent/progressive/refractory malignant glioma, stratum A	7	29		
Recurrent/progressive/refractory intrinsic BSG, stratum B	4	17.6		
Recurrent or progressive medulloblastoma, stratum C	2	8.3		
Recurrent or progressive ependymoma, stratum D	2	8.3		
Recurrent or progressive LGG, stratum E	9	37.5		
Age at diagnosis	24		10.82	0.35–18.54
MR parameters: permeability and CBV				
Kps_{max}				
Baseline	21		6.32	0.97–27.54
On treatment	12		4.8	1.11–25.23
Difference (baseline – on treatment)	9		3.02	–5.79 to 16.05
CBV_{max}				
Baseline	20		12.35	5.27–119.51
On treatment	12		16.56	1.5–58.44
Difference (baseline – on treatment)	9		4.59	–12.66 to 61.07
PET parameters: ^{18}F-FDG uptake ratio				
T/W_{max}				
Baseline	21		2.19	1.03–8.79
On treatment	12		1.77	1.22–3.06
Difference (baseline – on treatment)	9		0.68	–0.01 to 1.83

(http://www.sph.sc.edu/comd/rorden/mri-cro.html), a statistical parametric mapping tool for viewing medical images (*16*). Holodny et al. coregistered MR diffusion and PET images through the application of a 6-parameter rigid-body transformation matrix, followed by trilinear interpolation (*17*). Each transformation matrix was determined by a nonlinear gradient search for a maximum normalized mutual information cost function applied to the voxel intensities of each registered 3D image pair. ROIs were manually drawn on both MR and PET images using software from the McConnell Brain Imaging Centre of the Montreal Neurologic Institute. To effectively investigate the correlation between MR and PET in pediatric brain tumors, the registration of MR with PET images using a common ROI that can be applied to both studies is desirable.

In our study, we evaluated the feasibility of registering MR permeability and ^{18}F-FDG PET images using a common ROI. MR and PET images were acquired on separate scanners, and fused PET/MR images were obtained. Although either T1 perfusion images or T2* gradient images could have been used, the PET images were registered with the last time point of the T1 perfusion time series instead of T2* gradient images to minimize susceptibility artifacts that can be present with T2* acquisitions (*18*). Our results suggest that this automated registration method can be used successfully to transfer an ROI manually drawn on MR permeability images to ^{18}F-FDG PET images.

MR permeability can be used to assess vascular integrity. High-grade malignancy is often associated with increased macrovasculature and microvasculature and higher capillary leakage. Roberts et al. reported that in 22 patients aged 14–79 y with gliomas, MR permeability was correlated with pathologic grade (*19*). Law et al. reported that vascular permeability was correlated with tumor grade in 73 patients aged 4–85 y with primary gliomas, although the correlation was not as strong as expected (*20*). Several MR parameters can be used to evaluate tumor vascularity. Indeed, in the study by Law et al. (*20*), there was a stronger correlation between relative CBV (rCBV) and tumor grade than vascular permeability and tumor grade, suggesting that these parameters characterize different aspects of tumor physiology. The use of complementary MR parameters has been proposed

TABLE 2
Comparison of Baseline Imaging Parameters for Pediatric HGG/BSG with LGG

Imaging parameters	Tumor type	*n*	Minimum	Median	Maximum	*P**
Baseline Kps_{max}	HGG/BSG†	10	1.20	5.68	27.54	0.56
	LGG‡	7	0.97	6.63	20.73	
Baseline CBV_{max}	HGG/BSG†	9	7.80	25.04	119.51	0.081
	LGG‡	7	7.14	8.76	20.79	
Baseline T/W_{max}	HGG/BSG†	10	1.03	2.22	8.79	0.63
	LGG‡	7	1.44	2.05	2.88	

*Wilcoxon–Mann–Whitney Test.
†Stratum A and B.
‡Stratum E.

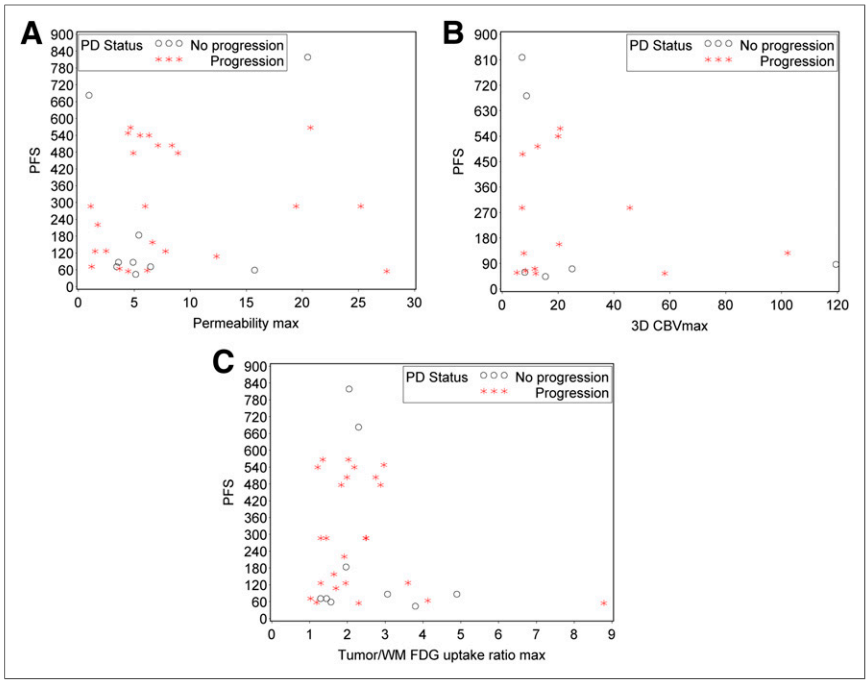

FIGURE 3. (A) Association between MR permeability and PFS. Permeability Kps_{max} was not significantly associated with PFS (P = 0.42, HR = 0.97, n_{events} = 15). (B) Association between 3D CBV_{max} and PFS. Three-dimensional CBV_{max} was not significantly associated with PFS (P = 0.41, HR = 0.989, n_{events} = 14). (C) Association between ^{18}F-FDG uptake and PFS. T/W_{max} ^{18}F-FDG uptake ratio was not significantly associated with PFS (P = 0.17, HR = 1.49, n_{events} = 15). max = maximum; PD = progressive disease.

for the evaluation of pediatric brain tumors (*21*), and it is possible that a combination of imaging parameters could be superior to any single parameter for tumor characterization. Indeed, Law et al. concluded that the combination of rCBV and vascular transfer constant was the best set of metrics to predict glioma grade but did not provide additional predictive value over rCBV alone (*22*).

Results in the literature on ^{18}F-FDG PET in adult brain tumors report that more intense uptake suggests increased tumor malignancy (*2*), aggressiveness (*3*), grade (*4,5*), and cell density (*6*). Delbeke et al. retrospectively reviewed 58 patients with histologically proven brain tumors aged 2–81 y (mean age ± SD, 38 ± 25 y) referred for baseline ^{18}F-FDG PET. A tumor–to–white matter ratio greater than 1.5 suggested high-grade disease, with a sensitivity of 94% and specificity of 77% (*7*). Barker et al. reported that more intense uptake was a significant predictor of poor survival in 55 patients with malignant glioma aged 11–65 y (median age, 45 y) (*8*). Patronas et al. (*9*) and Padma et al. (*10*) suggested PET could be used as a prognostic tool for survival.

Initial studies of ^{18}F-FDG PET in children with brain tumors have suggested that intensely ^{18}F-FDG–avid disease and extensive ^{18}F-FDG uptake is associated with a higher histologic grade and worse outcome. Kwon et al. found that in 12 children (age range, 3–14 y), intense ^{18}F-FDG uptake was more common in glioblastoma, whereas mild or no ^{18}F-FDG uptake was more common in anaplastic astrocytomas or low-grade astrocytomas (*23*). Williams et al. found that in 12 children (age range, 4.6–17.4 y), 3D maximum and mean tumor ^{18}F-FDG uptake were associated with PFS in supratentorial anaplastic astrocytomas when using 3D PET analysis techniques (*11*). Kruer et al. reported that in 46 children (age range, 4 mo to 18 y) with low-grade astrocytomas, ^{18}F-FDG PET and proliferation index were independent useful measures in the risk stratification of disease (*24*). Pirotte et al. found that in 20 children (age range, 1–13 y), ^{18}F-FDG PET guidance improved the diagnostic yield of stereotactic biopsy in newly diagnosed BSG and could have prognostic value (*25*). Gururangan et al. found that in 22 children (age range, 2.8–25 y) with either recurrent or newly diagnosed medulloblastoma there was a significant negative correlation between increased ^{18}F-FDG uptake and survival (*26*). Holthoff et al. found that ^{18}F-FDG uptake was found to be increased in patients with medulloblastoma, compared with other posterior fossa tumors (*27*). Borgwardt et al. found that in 38 children (age range, 0–16 y) with primary central nervous system tumors, increased ^{18}F-FDG uptake reflected histologic grade and that ^{18}F-FDG PET and MR coregistration improved tumor characterization (*1*). Of note, Borgwardt et al. performed both imaging with ^{18}F-FDG PET and imaging with ^{15}O-labeled water in 16 patients and found no correlation between cerebral blood flow and malignancy or cerebral blood flow and glucose metabolism.

Through the PBTC, we recently evaluated associations between MR imaging and ^{18}F-FDG PET in pediatric diffuse intrinsic BSG (*12*). If ^{18}F-FDG uptake was hyperintense, compared with gray matter, and was found in 50% or more of the tumor, survival was poor. We found an association of tumor diffusion values with uniformity of ^{18}F-FDG uptake, suggesting that increased tumor cellularity represents a greater number of viable tumor cells and higher ^{18}F-FDG uptake throughout the tumor. This finding agreed with reports by Palumbo et al. and Holodny et al. showing a correlation between lower apparent diffusion coefficient and increased ^{18}F-FDG uptake (*16,17*). Further, we suggested that higher ^{18}F-FDG uptake was associated with tumor enhancement, possibly reflecting more aggressive disease because most BSGs do not enhance (*28*).

The 24 children with brain tumors included in this study underwent both MR and ^{18}F-FDG PET as part of a multiinstitutional phase II study of bevacizumab and irinotecan therapy. When we compared MR and PET across the spectrum of pediatric brain tumors, we found that there was no significant correlation of baseline Kps_{max} with T/W_{max}, although our sample size was small. This lack of correlation could reflect the fact that T1 permeability on MR and ^{18}F-FDG uptake on PET measure different aspects of tumor physiology and may be complementary rather than correlative. Specifically, T1 permeability characterizes changes in vascular leakage associated with angiogenesis whereas ^{18}F-FDG uptake is associated with cellular glucose metabolism where ^{18}F-FDG freely crosses the blood–brain barrier. Of note, children with supratentorial HGG had slightly higher correlation than children with LGG, suggesting that correlation of Kps_{max} with T/W_{max} may also depend on tumor histology. However, a larger number of patients would be needed for a covariate analysis of Kps_{max}, T/W_{max}, and PFS by tumor histology. We found that baseline Kps_{max} was not

TABLE 3
Change in MR Permeability and ^{18}F-FDG Uptake Ratio at Baseline and on Treatment

Age (y)	Sex	Phase	Stratum (histology)	Kps_{max}	T/W_{max}	3D CBV_{max}
16.5	F	Baseline	A*	4.900	4.898	119.506
		Follow-up	A	3.593	3.065	58.44
15.8	F	Baseline	A	19.440	2.485	45.73
		Follow-up	A	25.227	2.499	58.394
12.7	F	Baseline	B†	7.799	1.957	7.799
		Follow-up	B	1.503	1.297	1.503
3.3	F	Baseline	B	6.459	1.451	25.04
		Follow-up	B	3.441	1.293	18.959
17.5	F	Baseline	C‡	8.354	2.752	12.68
		Follow-up	C	7.121	1.991	14.156
14.2	M	Baseline	E§	5.975	1.443	7.148
		Follow-up	E	1.115	1.298	2.561
5.9	F	Baseline	E	20.726	2.029	20.79
		Follow-up	E	4.678	1.352	7.13
3.6	F	Baseline	E	8.913	2.881	7.32
		Follow-up	E	4.916	1.839	11.664
10.3	M	Baseline	E	6.315	2.185	20.062
		Follow-up	E	5.520	1.216	20.814

*A, recurrent/progressive/refractory malignant glioma.
†B, recurrent/progressive/refractory intrinsic BSG.
‡C, recurrent or progressive medulloblastoma.
§E, recurrent or progressive LGG.

significantly associated with CBV_{max}, whereas baseline CBV_{max} was significantly associated with T/W_{max}. Because radiotracer uptake is related to the delivery of radiotracer to the tumor, which in turn is reflected by blood flow and CBV, this result was not unexpected. Further, we found that CBV_{max} was slightly higher in the cohort of children with HGG and BSG than in those with LGG. This correlation likely reflects the correlation of higher grade tumors with increased CBV_{max}. There was no such association of tumor type with vascular permeability or ^{18}F-FDG uptake. This result could be in part related to our small sample size. Law et al. previously suggested that there was a stronger correlation between rCBV and tumor grade than vascular permeability and tumor grade (*20*); therefore, there is a possibility that although our sample size was sufficiently large to show an association with CBV_{max}, it was not sufficient to show an association with Kps_{max} or T/W_{max}. Finally, T1 permeability and CBV were not significantly associated with PFS. ^{18}F-FDG uptake also was not significantly associated with PFS; however, there was a suggestion that such an association may be shown with an increase in the number of subjects.

The main limitations of this study were the small sample size and the mixture of tumor types. However, this was an exploratory evaluation of the feasibility of an approach for combining ^{18}F-FDG PET with MR permeability images after independent acquisition in the pediatric population that resulted in good to excellent coregistration of the tumor ROI across a spectrum of new and recurrent disease. In future studies, a multivariate analysis of both MR and PET parameters with PFS would be helpful using this approach in a homogeneous histologic group. However, there were not sufficient numbers of subjects in this preliminary investigation to test such a hypothesis. Future studies could also investigate associations of MR imaging with ^{18}F-FDG PET on hybrid PET/MR systems or the benefits of other PET radiopharmaceuticals such as ^{11}C-labeled methionine, ^{18}F-labeled choline, or ^{18}F-labeled fluorothymidine, among others. In addition, we used a simple ROI analysis to illustrate proof-of-principle that there is good anatomic correlation between the ^{18}F-FDG PET and MR permeability in a heterogeneous group of pediatric brain tumors. However, voxel-based analysis could also be considered in future expanded studies using this approach to characterize tumor tissue, to possibly identify active tumor regions and to monitor changes during therapy.

CONCLUSION

MR permeability and ^{18}F-FDG PET images were successfully registered across a spectrum of pediatric brain tumors using a common ROI applied to both studies. Subsequently, MR permeability and PET parameters were compared in this patient population. Although the lack of correlation between ^{18}F-FDG uptake on PET and MR permeability likely indicates these show different aspects of tumor physiology, correlation of ^{18}F-FDG uptake and CBV is likely due, at least in part, to the mechanism of radiotracer uptake and association with tumor grade. A larger number of patients is needed for a covariate analysis of these parameters and PFS by tumor histology.

DISCLOSURE

The costs of publication of this article were defrayed in part by the payment of page charges. Therefore, and solely to indicate this fact, this article is hereby marked "advertisement" in accordance with 18 USC section 1734. This work was supported in part by NIH grant U01 CA81457 for the Pediatric Brain Tumor Consortium (PBTC), the Pediatric Brain Tumor Consortium Foundation (PBTCF), the Pediatric Brain Tumor Foundation of the United States (PBTFUS), and American Lebanese Syrian Associated Charities. No other potential conflict of interest relevant to this article was reported.

ACKNOWLEDGMENT

We acknowledge Cynthia Dubé for her help with the manuscript preparation.

REFERENCES

1. Borgwardt L, Højgaard L, Carstensen H, et al. Increased fluorine-18 2-fluoro-2-deoxy-D-glucose (FDG) uptake in childhood CNS tumors is correlated with malignancy grade: a study with FDG positron emission tomography/magnetic resonance imaging coregistration and image fusion. *J Clin Oncol.* 2005;23:3030–3037.
2. Di Chiro G, DeLaPaz RL, Brooks RA, et al. Glucose utilization of cerebral gliomas measured by (^{18}F) fluorodeoxyglucose and positron emission tomography. *Neurology.* 1982;32:1323–1329.
3. Alavi JB, Alavi A, Chawluk J, et al. Positron emission tomography in patients with glioma: a predictor of prognosis. *Cancer.* 1988;62:1074–1078.
4. Kaschten B, Stevenaert A, Sadzot B, et al. Preoperative evaluation of 54 gliomas by PET with fluorine-18-fluorodeoxyglucose and/or carbon-11-methionine. *J Nucl Med.* 1998;39:778–785.
5. Ogawa T, Inugami A, Hatazawa J, et al. Clinical positron emission tomography for brain tumors: comparison of fludeoxyglucose F 18 and L-methyl-^{11}C-methionine. *AJNR.* 1996;17:345–353.
6. Herholz K, Pietrzyk U, Voges J, et al. Correlation of glucose consumption and tumor cell density in astrocytomas: a stereotactic PET study. *J Neurosurg.* 1993;79:853–858.
7. Delbeke D, Meyerowitz C, Lapidus RL, et al. Optimal cutoff levels of F-18 fluorodeoxyglucose uptake in the differentiation of low-grade from high-grade brain tumors with PET. *Radiology.* 1995;195:47–52.
8. Barker FG II, Chang SM, Valk PE, et al. 18-fluorodeoxyglucose uptake and survival of patients with suspected recurrent malignant glioma. *Cancer.* 1997;79:115–126.

9. Patronas NJ, Di Chiro G, Kufta C, et al. Prediction of survival in glioma patients by means of positron emission tomography. *J Neurosurg.* 1985;62:816–822.
10. Padma MV, Said S, Jacobs M, et al. Prediction of pathology and survival by ^{18}F-FDG PET in gliomas. *J Neurooncol.* 2003;64:227–237.
11. Williams G, Fahey F, Treves ST, et al. Exploratory evaluation of two-dimensional and three-dimensional methods of ^{18}F-FDG PET quantification in pediatric anaplastic astrocytoma: a report from the Pediatric Brain Tumor Consortium (PBTC). *Eur J Nucl Med Mol Imaging.* 2008;35:1651–1658.
12. Zukotynski KA, Fahey FH, Kocak M, et al. Diffuse intrinsic brain stem glioma: a report from the pediatric brain tumor consortium. *J Nucl Med.* 2011;52:188–195.
13. Poussaint TY, Philips PC, Vajapeyam S, et al. The Neuroimaging Center of the Pediatric Brain Tumor Consortium: collaborative neuroimaging in pediatric brain tumor research—a work in progress. *AJNR.* 2007;28:603–607.
14. Fahey FH, Kinahan PE, Doot RK, et al. Variability in PET quantitation within a multicenter consortium. *Med Phys.* 2010;37:3660–3666.
15. Mulkern RV, Forbes P, Dewey K, et al. Establishment and results of a magnetic resonance quality assurance program for the pediatric brain tumor consortium. *Acad Radiol.* 2008;15:1099–1110.
16. Palumbo B, Angotti F, Marano G. Relationship between PET-^{18}F-FDG and MR imaging apparent diffusion coefficients in brain tumors. *Q J Nucl Med Mol Imaging.* 2009;53:17–22.
17. Holodny A, Makeyev S, Beattie J, et al. Apparent diffusion coefficient of glial neoplasms: correlation with fluorodeoxyglucose-positron-emission tomography and gadolinium-enhanced MR imaging. *AJNR.* 2010;31:1042–1048.
18. Hackländer T, Reichenbach JR, Mödder U. Comparison of cerebral blood volume measurements using the T1 and T2* methods in normal human brains and brain tumors. *J Comput Assist Tomogr.* 1997;21:857–866.
19. Roberts HC, Roberts TP, Brasch RC, et al. Quantitative measurements of microvascular permeability in human brain tumors achieved using dynamic contrast-enhanced MR imaging: correlation with histologic grade. *AJNR.* 2000;21:891–899.
20. Law M, Yang S, Babb J, et al. Comparison of cerebral blood volume and vascular permeability from dynamic susceptibility contrast-enhanced perfusion MR imaging with glioma grade. *AJNR.* 2004;25:746–755.
21. Poussaint TY, Rodriguez D. Advanced neuroimaging of pediatric brain tumors: MR diffusion, MR perfusion, and MR spectroscopy. *Neuroimaging Clin N Am.* 2006;16:169–192.
22. Law M, Young R, Babb J, et al. Comparing perfusion metrics obtained from a single compartment versus pharmacokinetic modeling methods using dynamic susceptibility contrast-enhanced perfusion MR imaging with glioma grade. *AJNR.* 2006;27:1975–1982.
23. Kwon JW, Kim I, Cheon J, et al. Paediatric brainstem gliomas: MR imaging, ^{18}F-FDG-PET and histological grading correlation. *Pediatr Radiol.* 2006;36:959–964.
24. Kruer MC, Kaplan AM, Etzl MM, et al. The value of positron emission tomography and proliferation index in predicting progression in low-grade astrocytomas of childhood. *J Neurooncol.* 2009;95:239–245.
25. Pirotte BJ, Lubansu A, Massager N, Wikler D, Goldman S, Levivier M. Results of positron emission tomography guidance and reassessment of the utility of and indications for stereotactic biopsy in children with infiltrative brainstem tumors. *J Neurosurg.* 2007;107:392–399.
26. Gururangan S, Hwang E, Herendon JE II, Fuchs H, George T, Coleman RE. [^{18}F] fluorodeoxyglucose-positron emission tomography in patients with medulloblastoma. *Neurosurgery.* 2004;55:1280–1288.
27. Holthoff VA, Herholz K, Berthold F, et al. In vivo metabolism of childhood posterior fossa tumors and primitive neuroectodermal tumors before and after treatment. *Cancer.* 1993;72:1394–1402.
28. Fischbein NJ, Prados M, Wara W, Russo C, Edwards M, Barkovich A. Radiologic classification of brain stem tumors: correlation of magnetic resonance imaging appearance with clinical outcome. *Pediatr Neurosurg.* 1996;24:9–23.